Aramid/poly(ether sulphone) blend: crystallization accelerated by the presence of amorphous polymer

Motoshi Matsuura, Hiromu Saito, Shoichi Nakata, Yoshio Imai and Takashi Inoue*

Department of Organic and Polymeric Materials, Tokyo Institute of Technology, Ookayama, Meguro-ku, Tokyo 152, Japan

(Received 14 February 1991; revised 19 September 1991; accepted 26 September 1991)

An aramid, prepared by the polycondensation of bis(4-aminophenyl) ether with isophthaloyl chloride, was found to render a single-phase mixture with poly(ether sulphone) (PES) by solution casting. Crystallization of the blend was studied by wide-angle X-ray diffraction, H_V light scattering, differential scanning calorimetry, Fourier-transform infra-red spectroscopy and scanning electron microscopy. The crystallization of aramid was found to be accelerated dramatically by adding PES, e.g. the crystallization rate constant of a 50/50 blend was shown to be one decade higher than that of neat aramid at around 310°C. The accelerated crystallization was ascribed to the elevation of chain mobility of aramid by blending with PES. It may be caused by the decrease of T_g via blending of a low-T_g component (PES), but this contribution was estimated to be small. The major contribution seems to be due to the partial dissociation of aramid–aramid interactions and the 'up-hill diffusion' associated with the liquid–liquid phase separation.

(Keywords: polymer blend; aramid; poly(ether sulphone); crystallization; acceleration; chain mobility; interaction; liquid–liquid phase separation)

INTRODUCTION

It is well known that the crystallization rate of a crystalline polymer is reduced on mixing with an amorphous polymer. Typical examples are seen in poly(vinylidene fluoride) (PVDF)/poly(methyl methacrylate) (PMMA)[1,2], poly(ε-caprolactone)/poly(vinyl chloride)[3], PVDF/poly(ethyl acrylate)[4], and poly(ethylene oxide)/PMMA[5] systems. In contrast, we recently found that a single-phase mixture of aramid PA44I:

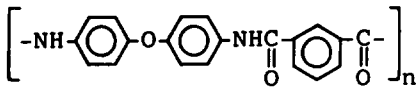

and poly(ether sulphone) (PES) exhibits interesting crystallization behaviour[6]: the aramid can crystallize in the blend, whereas it had been thought to be an amorphous polymer[7]. That is, the aramid seems to be a dormant crystalline polymer and the crystallization is induced or accelerated by the presence of amorphous polymer (PES).

Following the preliminary results mentioned above, in this paper we investigate the details of the crystallization by wide-angle X-ray diffraction (WAXD), H_V light scattering (LS), differential scanning calorimetry (d.s.c.), Fourier transform infra-red spectroscopy (*FT*i.r.) and scanning electron microscopy (SEM) to confirm further the blend-induced or blend-accelerated crystallization and discuss the mechanism.

EXPERIMENTAL

Aramid PA44I was prepared by a low-temperature solution polycondensation of bis(4-aminophenyl) ether with isophthaloyl chloride in *N*,*N*-dimethylacetamide (DMAc). PES was supplied by Imperial Chemical Industries (Victrex 300P). The intrinsic viscosities of the aramid and PES in DMAc at 30°C were 1.54 and 0.43 dl g^{-1}, respectively.

The aramid and PES were dissolved at 3 wt% of total polymer in DMAc. The solution was poured into a large volume of methanol and precipitated. The precipitates were collected and washed thoroughly with hot methanol for 30 min, and were then dried under a vacuum of 10^{-2} mmHg at room temperature for 24 h and at 80°C for 24 h. The blend powder thus obtained was compression-moulded at T_g + 100°C into a thick film (ca. 1 mm thick). The thick film was used for WAXD study. A thin film of ca. 40 μm thickness was also prepared by solution casting; the solution was cast on a cover glass and dried under reduced atmosphere (10^{-4} mmHg), first at 20°C for 24 h, then at 100°C for 24 h and further at 230°C for 24 h. The cast film was used for the light scattering and d.s.c. experiments. For infra-red spectroscopy, a very thin film (ca. 10 μm thick) was prepared by casting a 3 wt% DMAc solution onto a KBr disc and drying in the same way.

The thick film was inserted into a hot stage set at the desired annealing (crystallization) temperature under a nitrogen atmosphere. After annealing, the specimen was quickly quenched to room temperature to freeze the structure developed during annealing. The WAXD

*To whom correspondence should be addressed

0032-3861/92/153210-05

profile of the annealed quenched specimen was observed on a Rigakudenki RU-200 X-ray diffraction apparatus using nickel-filtered Cu K_α radiation (50 kV, 180 mA).

Real-time analysis on the crystallization by LS was carried out by placing the thin film on a cover glass in a hot chamber kept at the desired crystallization temperature and by annealing isothermally under a N_2 atmosphere. The chamber was set horizontally on the light scattering stage. A polarized He–Ne gas laser beam of 632.8 nm wavelength was applied vertically to the film specimen. The scattered light was passed through an analyser set at the crossed nicols state for the incident light, i.e. at the H_V geometry[8]. The angular distribution of H_V light scattering intensity was detected by a one-dimensional photometer with an array of 46 photodiodes (HASC Corp.).

Fourier-transform infra-red spectroscopy (*FT*i.r.) was carried out by an FT-IR/5000 spectrometer with 4 cm^{-1} resolution (Japan Spectroscopic Co. Ltd).

Two-phase morphology in the annealed quenched blend was observed under a scanning electron microscope (model JSM-T200, JEOL Ltd). For SEM observation, the specimen was fractured in liquid nitrogen and rinsed with chloroform (good solvent for PES).

The d.s.c. thermograms were recorded by a du Pont 910 DSC at a heating rate of 20°C min^{-1}.

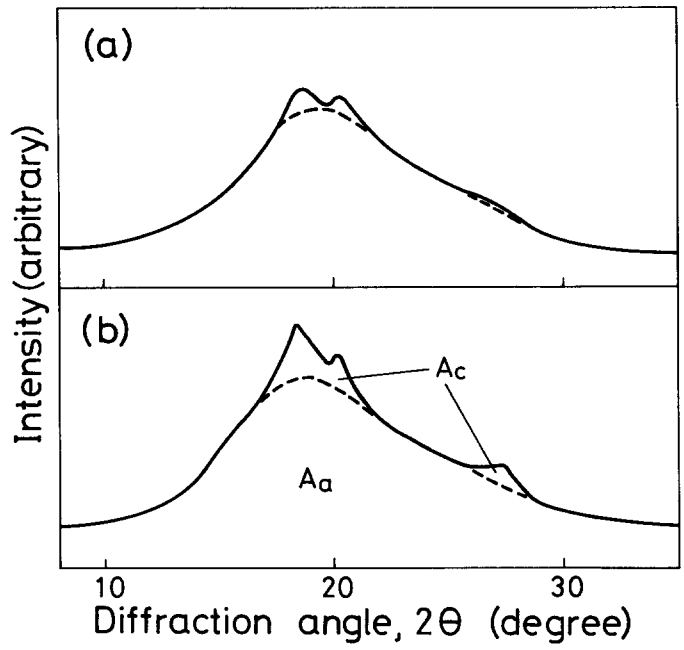

Figure 2 Wide-angle X-ray diffraction profiles: (a) aramid and (b) 50/50 aramid/PES. The full curve is for the specimen annealed at 320°C for 120 min and the broken curve for the unannealed specimen

RESULTS AND DISCUSSION

The observed d.s.c. thermograms are shown in *Figure 1*. Curves A and B show that neat PES and aramid have glass transition temperatures (T_g) at 220 and 264°C, respectively. A 70/30 aramid/PES blend shows a single T_g intermediate between those of the constituents (curve C), indicating the single-phase nature in the cast film of the blend. The 70/30 blend also shows a clear exothermic peak at around 330°C. It could be assigned to the crystallization of aramid. A thermogram in the second run (curve D) after the first run up to 350°C shows two T_g values. It suggests that phase decomposition had taken place during the first run. A blend annealed at 300°C for 12 h shows the low T_g based on PES but no clear high T_g (curve E). The high T_g seems to have disappeared because crystallization has proceeded to reduce the remaining amorphous aramid to a negligible level.

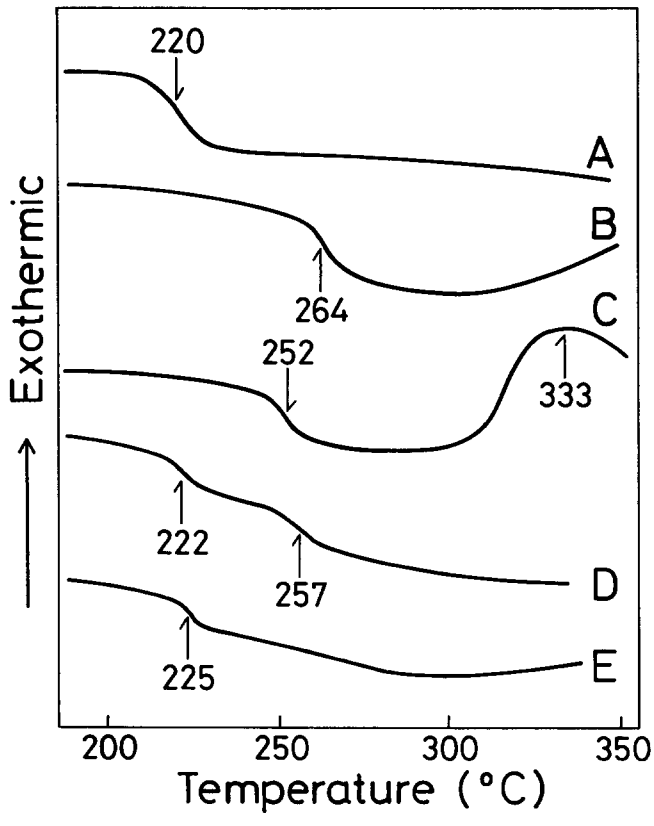

Figure 1 D.s.c. thermograms for neat polymers and a 70/30 aramid/PES blend: (A) PES, (B) aramid, (C) unannealed blend in the first scan, (D) unannealed blend in the second scan, and (E) the blend annealed at 320°C for 5 h

The crystallization of aramid can be confirmed by the WAXD analysis. In *Figure 2* are shown the WAXD profiles of (a) neat aramid and (b) a 50/50 aramid/PES blend, both annealed at 320°C for 2 h. Here also the profiles of the unannealed specimens are shown by broken curves. Both annealed specimens show definite diffraction peaks at diffraction angles $2\theta = 18.5°$, 20° and 27°. It indicates that the neat aramid can crystallize by annealing for a long time, whereas it had been thought to be an amorphous polymer[7]. The diffraction angles of the blend are identical to those of the neat aramid, suggesting that the aramid crystallizes in the blend. Most interesting is that the peak area of the blend is much larger than that of neat aramid. It suggests that the crystallization of aramid is accelerated by adding PES.

To estimate the degree of crystallinity, we calculated the ratio of the peak area between full and broken curves (A_c, see *Figure 2b*) to that below the full curve ($A_c + A_a$) in a limited range of 2θ ($8° \leqslant 2\theta \leqslant 35°$), i.e. $A_c/(A_c + A_a)$. For the blends, the ratio was divided by the weight fraction of aramid w_1. The normalized crystallinity of aramid component, $X = A_c/(A_c + A_a)w_1$, is plotted as a function of the annealing time in *Figure 3*. The crystallinity increases with annealing time in both neat aramid and blend. The higher the PES content, the faster is the crystallization. It confirms that the crystallization

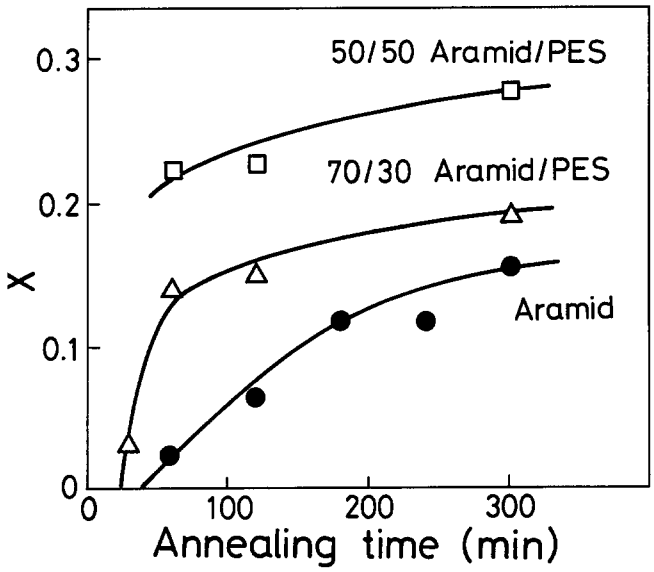

Figure 3 Crystallinity by WAXD *versus* annealing time at 320°C

of aramid is accelerated by adding the amorphous polymer. The results in *Figures 2* and *3* are on the annealed quenched specimens. Accelerated crystallization can be further confirmed on the basis of a real-time investigation by the H_V light scattering as follows.

The H_V light scattering patterns from the crystallized specimens were circular symmetric, i.e. there was no azimuthal angle dependence. It suggests that the orientation fluctuation is randomly correlated. In the case of random orientation correlation, one can analyse the crystallinity in terms of the integrated scattering intensity, i.e. the invariant Q_{H_V} defined by[9]:

$$Q_{H_V} = \int_0^\infty I(h)h^2\,dh \tag{1}$$

where I is the intensity of scattered light and h is the magnitude of the scattering vector, $h = (4\pi/\lambda)\sin(\theta/2)$, λ and θ being the wavelength of the light and the scattering angle, respectively. For a two-phase system containing anisotropic crystallites dispersed in an isotropic matrix, the invariant Q_{H_V} is given by[9]:

$$Q_{H_V} \propto \phi_c(\alpha_1 - \alpha_2)^2 \tag{2}$$

where ϕ_c is the volume fraction of crystallite and $(\alpha_1 - \alpha_2)$ is the optical anisotropy in terms of the polarizability difference between the principal axes of the crystallite.

The time variation of the invariant Q_{H_V} at 320°C is shown in *Figure 4*. The time variations of various systems are quite similar to those by WAXD in *Figure 3*. Thus the accelerated crystallization is supported by the real-time observation.

Once the relationship between Q and the degree of crystallization by WAXD is given, one can discuss the crystallization kinetics more quantitatively in terms of the time variation of ϕ_c by the Avrami equation[10,11]:

$$1 - \phi_c = \exp(-kt^n) \tag{3}$$

where t is the crystallization time, and k and n are constants. As shown in *Figure 5*, plots of $\log[-\ln(1-\phi_c)]$ *versus* $\log t$ in the early stage of crystallization yielded a straight line as expected from equation (3). The n given by the slope in *Figure 5* is 1.0 ± 0.2. It suggests heterogeneous nucleation and one-dimensional crystal growth.

In the case of heterogeneous nucleation and one-dimensional growth, kt^n in equation (3) is given by[11]:

$$kt^n = NGt \tag{4}$$

where N is the number of nuclei per unit area and G is the lateral growth rate. From equations (3) and (4), the time t^* required to attain a crystallinity ϕ_c^* is described by:

$$(t^*)^{-1} = [-\ln(1 - \phi_c^*)]^{-1}NG \tag{5}$$

Hence we can employ $(t^*)^{-1}$ as a rate constant of crystallization[12,13]. We set $\phi_c^* = 0.07$, which is the midpoint of the straight region of the plots in *Figure 5*, and obtained $(t^*)^{-1}$. The temperature dependence of $(t^*)^{-1}$ is shown in *Figure 6*. The $(t^*)^{-1}$ values of the blends are higher than those of neat aramid below 320°C. The $(t^*)^{-1}$ value of the 50/50 blend at 310°C, for example, is shown to be about one decade higher than that of neat aramid.

Now, assuming that the temperature dependence of G is described by the Hoffman–Lauritzen theory on secondary nucleation[11,14,15], the rate constant $(t^*)^{-1}$ is formulated by:

$$(t^*)^{-1} \propto [-\ln(1 - \phi_c)]^{-1}N \underbrace{\exp\left(-\frac{Q_G}{R(T_c - T_g + 30)}\right)}_{\text{chain mobility}} \underbrace{\exp\left(-\frac{K_G}{T_c(\Delta T)f}\right)}_{\text{nucleation}} \tag{6}$$

where Q_G is the activation energy for transport across the liquid–crystal interface during secondary nucleation, R is the gas constant, T_c is the crystallization temperature, K_G is the nucleation constant for secondary nucleation, ΔT is the supercooling $(= T_m^\circ - T_c$, T_m° being the equilibrium melting temperature) and f is the correction factor given by $2T_c/(T_m^\circ + T_c)$. Equation (6) implies that, as T_c is lowered from T_m°, $(t^*)^{-1}$ increases and attains a maximum, and then it decreases when T_c approaches T_g. The increase at higher temperatures is mostly controlled

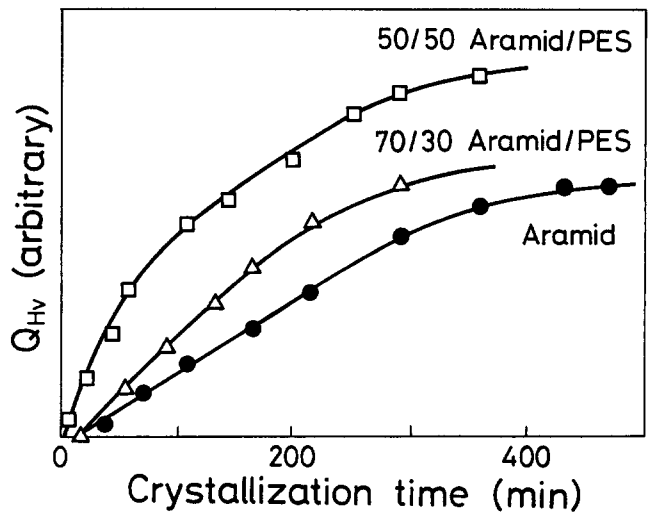

Figure 4 Time variation of the invariant of H_V scattered light at 320°C

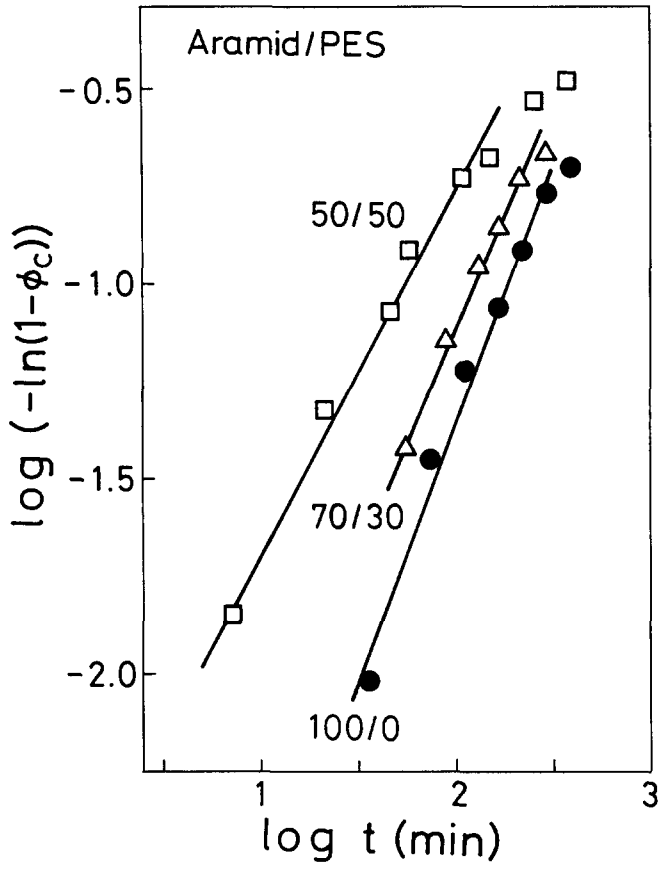

Figure 5 Avrami plot; crystallization at 320°C

by the nucleation term and the decrease at lower temperatures by the chain mobility term.

As shown in *Figure 6*, the crystallization rate constant $(t^*)^{-1}$ is lower at lower T_c. It implies that the crystallization is in the regime controlled by the chain mobility term.

Aramid has higher T_g than PES as shown in *Figure 1*. By blending with the lower T_g component, the chain mobility of aramid is expected to be elevated and hence $(t^*)^{-1}$ will increase. However, the increase estimated from the mobility term in equation (6) is rather small, e.g. about 280% increase in $(t^*)^{-1}$ for the 50/50 blend with $T_g = 252°C$. The increase is much smaller than that observed (ca. 950% increase). Thus, the simple T_g (or mobility) argument does not provide sufficient interpretation of the accelerated crystallization. Further, the simple T_g argument itself may be invalid if phase decomposition (discussed in *Figure 1*) precedes and crystallization follows. That is, once aramid chains are segregated from the single-phase mixture, the mobility of the segregated chains should be essentially the same as that of neat aramid and hence acclerated crystallization cannot be expected.

Concerning the chain mobility, one has to take account of the specific interchain interactions. In neat aramid, strong interchain interaction due to the hydrogen bonding between amide groups may exist and it will reduce the chain mobility. In the single-phase mixture, on the other hand, a dissociation of the hydrogen bonding is expected by the incorporation of PES. In *Figure 7* are shown the *FT*i.r. spectra of neat aramid and a 70/30 aramid/PES blend. The spectra are presented in a limited range of 3150–3450 cm^{-1}, since the whole spectrum of the blend

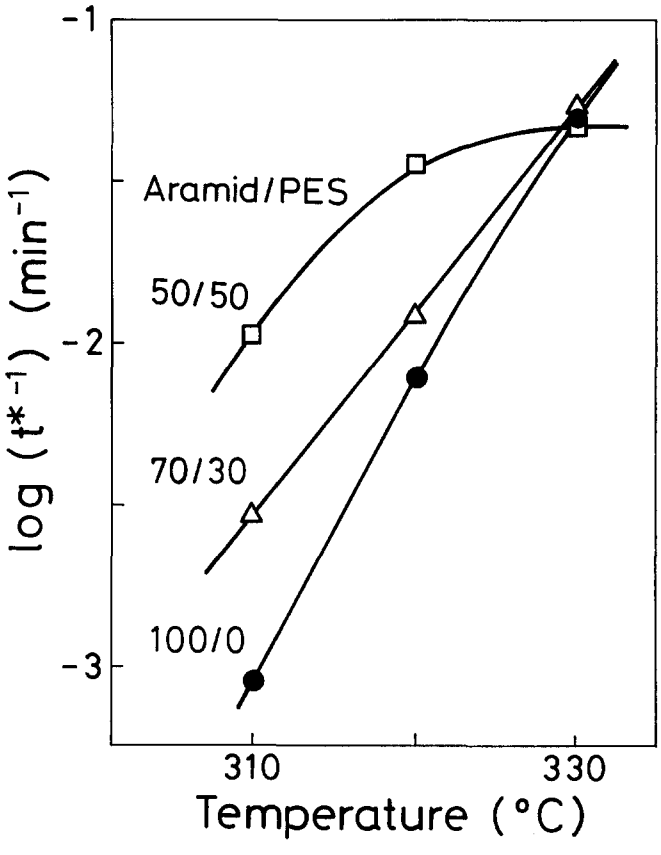

Figure 6 Temperature dependence of the crystallization rate constant $(t^*)^{-1}$

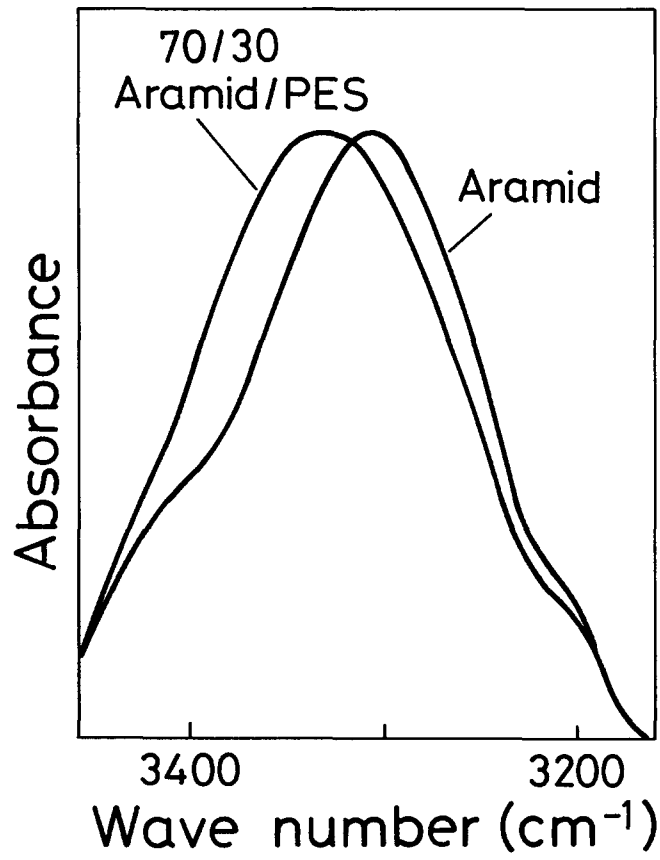

Figure 7 *FT*i.r. spectra covering the N–H stretching frequency range

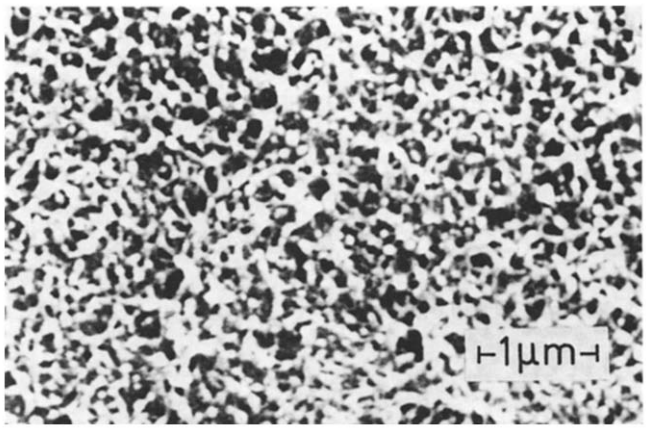

Figure 8 Scanning electron micrograph of the 70/30 aramid/PES annealed at 320°C for 5 h

did not show a dramatic deviation from the additive spectrum of the component polymers but a small, distinct deviation was observed only in the N–H stretching frequency region around 3300 cm^{-1}. The peak position shifts to higher frequency by blending with PES. It may imply that some of the aramid–aramid bonds dissociate to form aramid–PES bonds, which are slightly weaker than aramid–aramid bonds. Thus, spectroscopic analysis suggests the possibility for a mobility increase of aramid chains on blending with PES.

As discussed in *Figure 1*, annealing yields not only crystallization (liquid–solid phase separation) but also phase decomposition (liquid–liquid phase separation). It implies that the single-phase mixture prepared by solution casting (and also by precipitation and compression moulding) is in the non-equilibrium state, which has been frozen during the casting, so that, once the mixture is heated above T_g, phase decomposition proceeds. *Figure 8* shows a SEM micrograph of a well annealed blend. The SEM observation was carried out after solvent etching with chloroform so that the remaining material may be aramid. A highly interconnected aramid phase with unique periodicity is seen in the micrograph. Both the periodic character in the two-phase structure and the high level of phase interconnectivity seem to originate from spinodal decomposition.

It is well known that spinodal decomposition renders the periodic concentration fluctuation. The growth of concentration fluctuation is realized by the 'up-hill diffusion'; say, A molecules diffuse into A-rich regions from B-rich regions. So, in the aramid/PES system, aramid chains are forced to move from PES-rich regions to aramid-rich regions, in which crystallization takes place. In other words, the crystallizable chains are supplied to the crystal growth front under the thermodynamic driving force for phase separation; hence, the crystallization rate could be elevated. That is, liquid–liquid phase separation is expected to accelerate liquid–solid phase separation.

CONCLUSIONS

The crystallization of aramid was shown to be accelerated by adding the amorphous polymer PES. The acceleration seems to be caused by three contributions: the decrease in T_g by blending with a low-T_g component (PES), the partial dissociation of aramid–aramid interchain interactions, and the 'up-hill diffusion' associated with liquid–liquid phase separation. The crystallization and liquid–liquid phase separation may be competitive. The competitive situation will be quantitatively analysed and the results presented in the near future.

REFERENCES

1 Wang, T. T. and Nishi, T. *Macromolecules* 1977, **10**, 421
2 Saito, H., Okada, T., Hamane, T. and Inoue, T. *Macromolecules* 1991, **24**, 4446
3 Ong, C. J. and Price, F. P. *J. Polym. Sci., Polym. Symp.* 1978, **63**, 59
4 Alfonso, G. C. and Russell, T. P. *Macromolecules* 1986, **19**, 1143
5 Briber, R. M. and Khoury, F. *Polymer* 1987, **28**, 38
6 Nakata, S., Kakimoto, M., Imai, Y. and Inoue, T. *Polym. J.* 1990, **22**, 80
7 Kuze, K. and Miwa, S. *Kogyo Kagaku Zasshi* 1968, **71**, 443
8 Stein, R. S. and Rhodes, M. B. *J. Appl. Phys.* 1960, **31**, 1873
9 Koberstein, J., Russell, T. P. and Stein, R. S. *J. Polym. Sci., Polym. Phys. Edn.* 1979, **17**, 1719
10 Avrami, M. *J. Chem. Phys.* 1939, **7**, 1103; 1940, **8**, 212; 1941, **9**, 177
11 Wunderlich, B. 'Macromolecular Physics', Vol. 2, 'Crystal Nucleation, Growth, Annealing', Academic Press, New York, 1976
12 Stack, G. M., Mandelkern, L., Kröhnke, C. and Wegner, G. *Macromolecules* 1989, **22**, 4351
13 Fatou, J. G., Marco, C. and Mandelkern, L. *Polymer* 1990, **31**, 1685
14 Lauritzen, J. I. Jr and Hoffman, J. D. *J. Appl. Phys.* 1973, **44**, 4340
15 Hoffman, J. D., Frolen, L. J., Ross, G. S. and Lauritzen, J. I. Jr *J. Res. Nat. Bur. Stand. (A)* 1975, **79**, 671